

Nadia Galeotti¹
Fabian Jirasek¹
Jakob Burger^{2,*}
Hans Hasse¹

Recovery of Furfural and Acetic Acid from Wood Hydrolysates in Biotechnological Downstream Processing

Wood hydrolysates contain sugars that can be used as feedstock in fermentation processes. For that purpose, the hydrolysate must be concentrated and inhibitors that harm fermentation must be removed. Herein, the integration of these tasks with the recovery of inhibitors is studied. The wood hydrolysate is represented as a mixture of water, xylose, acetic acid, and furfural. Acetic acid and furfural are two frequently occurring inhibitors and valuable chemicals, and thus, their recovery is studied. Furfural is recovered from the vapors by heteroazeotropic distillation. It is shown that this can be achieved without additional energy. The recovery of acetic acid by distillation is also possible, but not attractive. The new process is simulated by using a thermodynamic model based on experimental data.

Keywords: Acetic acid, Furfural, Heteroazeotropic distillation, Wood hydrolysates

Received: May 25, 2018; *revised:* August 30, 2018; *accepted:* September 03, 2018

DOI: 10.1002/ceat.201800258

© 2018 The Authors. Published by Wiley-VCH Verlag GmbH & Co. KGaA. This is an open access article under the terms of the Creative Commons Attribution-NonCommercial-NoDerivs License, which permits use and distribution in any medium, provided the original work is properly cited, the use is non-commercial and no modifications or adaptations are made.

1 Introduction

The production of chemicals, polymers, and fuels from biomass is becoming increasingly important [1–3]. One of the most widely used biomass feedstocks is lignocellulosic biomass. It is available, e.g., in large amounts in the pulp and paper industry. Hydrolysates of lignocellulosic biomass contain sugars that can be used in fermentations that yield desired products, such as ethanol [4–8]. However, raw hydrolysates are not suited for fermentation; first, because the sugar concentration is too low and, second, because they contain components that are toxic for microorganisms, the so-called inhibitors. These inhibitors stem from the degradation of lignin and sugars in the pulping and prepulping operations. Some of the major inhibitors are carboxylic acids (mainly formic acid and acetic acid (AA)), furfural (F), and 5-hydroxymethylfurfural [9, 10]. Several detoxification methods are used for removing these inhibitors, in particular, evaporation, solvent extraction, adsorption, and anion exchange [9, 11–13]. Some of the inhibitors, e.g., AA and F, are valuable chemicals; therefore, it is interesting to recover them in high yield and purity [8, 12, 14]. One option to recover F is the use of heteroazeotropic distillation [12, 14, 15].

Herein, it is studied how F and AA can be recovered from the hydrolysate by heteroazeotropic distillation and how this can be combined suitably with increasing sugar concentration by evaporation. A model quaternary mixture composed of water (W), xylose (X), AA, and F is used to represent the hydrolysate. A thermodynamic model of this mixture was recently developed based on comprehensive experimental data on relevant mixtures [16]. The model is used herein as a basis

for process simulations. W and F have a miscibility gap; therefore, the model describes not only the vapor-liquid equilibrium (VLE), but also the liquid-liquid equilibrium (LLE) and the vapor-liquid-liquid equilibrium (VLLE). A new process is proposed that combines evaporation for the concentration step with heteroazeotropic distillation to recover F. No additional energy is needed for the recovery of F. The recovery of AA by distillation is possible, but not attractive.

2 Process Description

A scheme of the proposed process for the simultaneous concentration and detoxification of the hydrolysate and the recovery of F is shown in Fig. 1. Here, an overview of the process is given; details are specified below. The feed (stream FEED) is a dilute aqueous solution of X containing some AA and F and represents the raw hydrolysate. The concentration of X is increased in an evaporator (EVAP), which operates at 20.0 kPa to avoid the thermal degradation of the X. Herein, a single evaporation step is simulated, but for energy optimization

¹Nadia Galeotti, Fabian Jirasek, Prof. Dr.-Ing. Hans Hasse
University of Kaiserslautern, Laboratory of Engineering Thermodynamics (LTD), Erwin-Schrödinger Strasse 44, 67663 Kaiserslautern, Germany.

²Prof. Dr.-Ing. Jakob Burger
burger@tum.de
Technical University of Munich, Chair of Chemical Process Engineering, Campus Straubing for Biotechnology and Sustainability, 94315 Straubing, Germany.

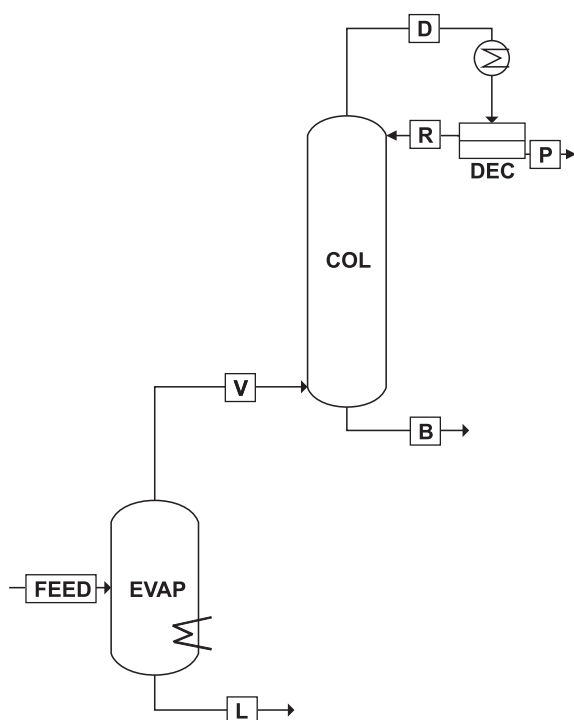


Figure 1. Process scheme for the recovery of F. Vapor from the evaporator (EVAP) is fed directly to the bottom of a rectification column (COL), which has no reboiler. B, bottom stream; D, distillate stream; DEC, decanter; L, liquid stream exiting the evaporator; P, product stream; R, reflux stream; V, vapor stream exiting the evaporator.

multi-effect evaporators are usually used in industrial processes. For the recovery of F from the vapor stream from the evaporator (stream V), heteroazeotropic distillation is used. Distillation is also performed at 20.0 kPa to facilitate integration with the evaporator. Lower pressures are undesired because they would increase the volumetric gas flow, which is already comparatively large for 20 kPa. Higher pressures would result in the need for a compressor because the gas leaving the evaporator is directly fed to the bottom of the distillation column (COL). Hence, COL has only a rectifying section and no stripping section. It also has no reboiler. The distillate stream at the top of the COL (stream D) has almost the composition of the heteroazeotrope in the system (W + F). It is condensed and then split in the decanter (DEC) into two liquid phases: the W-rich phase is recycled to the COL (stream R), whereas the other phase, which is rich in F, is the product (stream P). At the bottom of the COL, a dilute aqueous solution of AA is obtained (stream B). This process is called the *F recovery process* hereafter.

In a variant of this process shown in Fig. 2, AA is also recovered. For this purpose, a liquid side stream (stream S) is drawn from the COL: W leaves the COL mostly through this side stream, which additionally contains traces of F and AA. The bottom stream is AA of high purity. The F-rich top product is basically unchanged, relative to the process discussed above. This process is called the *F and AA recovery process* hereafter.

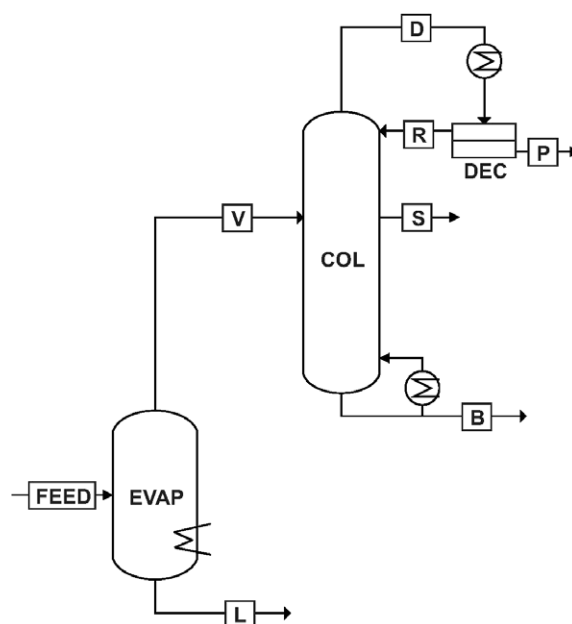


Figure 2. Process scheme for the recovery of F and AA. S, side draw.

3 Thermodynamic Model

Fig. 3 shows a scheme of the model of the VLE of the system (W + X + AA + F). X is present only in the liquid phases. The non-ideality of the liquid phases is described by the nonrandom two-liquid activity coefficient model (NRTL) [17]. The dimerization of AA is considered only in the vapor phase, which is ideal regarding physical interactions. The NRTL parameters resulting from the model are reported in Tab. 1. The parameters and correlation of the pure component vapor pressures used in the model are reported in Tab. 2. The dimerization reaction of AA in the vapor phase is considered as an equilibrium reaction. The equilibrium constant $K^{D, 1)}$ is determined by Eq. (1):

$$K^D = \frac{y_{\text{dimer}}}{(y_{\text{monomer}})^2} = \exp(-19.1001 + 7928.7/T) \quad (1)$$

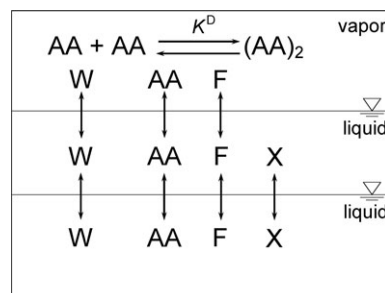


Figure 3. Scheme of VLE of the system (W + X + AA + F). The dimerization of AA is considered in the gas phase only.

1) List of symbols at the end of the paper.

Table 1. NRTL parameters used herein, $\tau_{ij} = a_{ij} + b_{ij}/T$ [16].

$i + j$	a_{ij} [-]	b_{ij} [K]	a_{ji} [-]	b_{ji} [K]	$\alpha_{ij} = \alpha_{ji}$ [-]
W + X	1.29480	0.000	-1.54200	0.000	0.30
W + AA	-11.37710	4318.650	7.29431	-2532.240	0.47
W + F	3.75496	-55.438	-3.21520	1221.700	0.30
X + AA	3.41027	0.000	2.24623	0.000	0.47
X + F	3.17074	0.000	6.51710	0.000	0.30
AA + F	0.67716	0.000	0.00045	0.000	0.47

Table 2. Parameters for the correlation of the pure component vapor pressures [16]. $\ln p_i^S = A_i + B_i/T + C_i \ln T + D_i T^{E_i}$

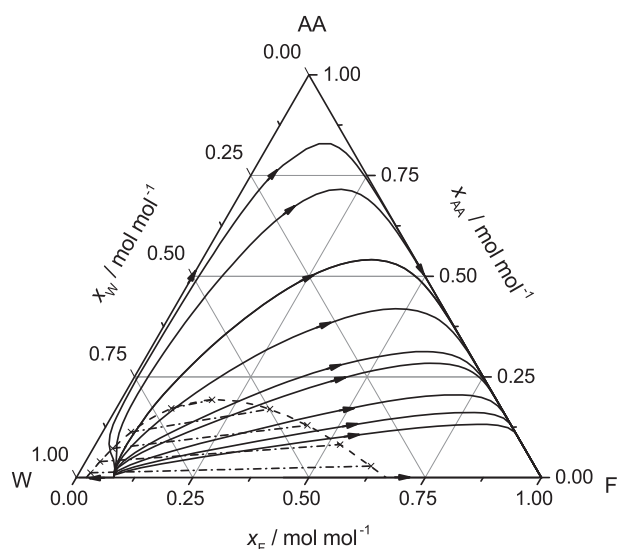
i	A_i	B_i	C_i	D_i	E_i
W	66.7412	-7258.2	-7.3037	0.41653×10^{-5}	2
AA	46.3622	-6304.5	-4.2985	0.88865×10^{-17}	6
F	87.6622	-8372.1	-11.1300	0.88150×10^{-2}	1

in which y_{dimer} and y_{monomer} denote the vapor-phase mole fractions of AA monomer and dimer, respectively. More information on the model and comparisons with experimental data are given in [16]. All simulations discussed herein are based on this model.

As a basis for the process design, the residue curve map for the ternary system (W + AA + F) at 20.0 kPa, as calculated by using the thermodynamic model, is shown in Fig. 4. It also includes information on the LLE at 298.15 K and 1 bar. The calculations were performed by using the Aspen Plus software [18]. The residue curves map of the ternary system has only a single distillation region. All residue curves start from the binary azeotrope (W + F) and end in pure F. Hence, F is the global high boiler; the azeotrope (W + F) is the global low boiler; and AA and W are saddle points, at which W is more volatile than AA. The feed stream of the distillation column is W-rich and contains only small amounts of AA and F. Therefore, pure F is not obtained in the bottom of the distillation column, but rather a W-rich stream, whereas, at the top of the column, the low-boiling azeotrope (W + F) is obtained. Upon condensation, it splits into two phases. The F-rich phase is withdrawn, and the other phase is used as reflux. The bottom product lies on the (W + AA) side of the phase diagram shown in Fig. 4, and is found from the feed and top product by using a material balance. In the F and AA recovery process, the side draw has to be added to the material balance.

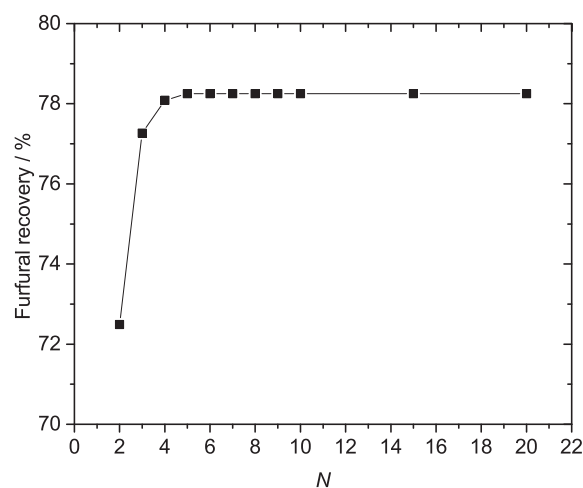
4 Process Model and Simulation Procedure

The simulation of the two process variants, the F recovery process (Fig. 1) and the F and AA recovery process (Fig. 2), is

**Figure 4.** Residue curves map (20.0 kPa), including the liquid-liquid phase envelope (298.15 K), for the ternary system (W + AA + F). Solid line, residue curve; dashed line, phase envelope; \times – \times , tie lines.

based on the equilibrium stage model. The evaporator, condenser, and reboiler (if present) were simulated as individual equilibrium stages. The condenser is a total condenser.

In the F recovery process (Fig. 1), the distillation column has one degree of freedom, namely, the number of stages N (heteroazeotropic distillation, no stripping section, no reboiler, for a given feed stream and pressure). Hence, the recovery of F depends only on the number of stages in the column. This dependency is shown in Fig. 5 for a typical column feed. It shows barely any change in the recovery of F for $N \geq 6$. For a safety margin, herein, the number of equilibrium stages of the distillation column was chosen to be $N = 8$. The operating point is discussed in the next section.

**Figure 5.** F recovery rate in the heteroazeotropic distillation of the F recovery process (cf. Fig. 1) as a function of the number of equilibrium stages N ($p = 20$ kPa, the column feed is specified in Tab. 3).

In the F and AA recovery process (Fig. 2), the distillation column has five degrees of freedom (heteroazeotropic distillation, stripping and rectifying section, reboiler, side draw, for a given feed stream and pressure). The five degrees of freedom are the number of stages in the rectifying and stripping section, the side-draw position, the side-draw flow rate, and the reboiler duty. The rectifying section of the column shown in Fig. 2 is essentially the same as that of the column shown in Fig. 1. The W-rich liquid side draw is taken from the stage on which the gaseous feed enters, which is also similar to the process shown in Fig. 1. The position of the side draw was found to be optimal at the height of the feed in preliminary simulations. However, in the process shown in Fig. 2, a large number of stages is needed in the stripping section of the column to achieve the desired purity of AA. The column design was performed by following the idea of the N - Q curve proposed in [19]. The N - Q curve is reported in Fig. 6 and it leads to $N = 28$, and feed (N_F) and side-draw (N_S) positions of $N_F = N_S = 20$ counting from the bottom. In the design, a compromise between the number of stages and the reboiler duty is made. The operating point is discussed in the next section. The simulations were performed with Aspen Plus [18]. The evaporation enthalpies and heat capacities of the pure components were obtained from the databank APV86.PURE32 included in Aspen Plus.

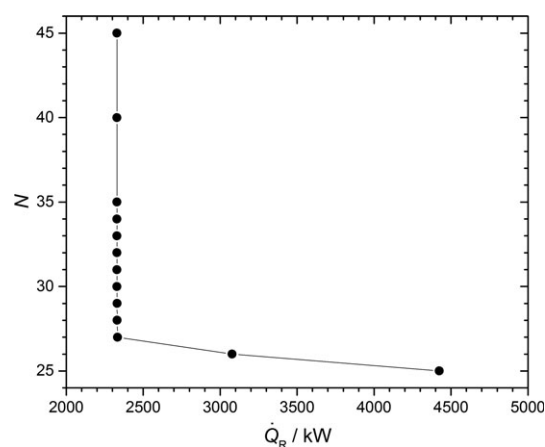


Figure 6. N - Q curve for the heteroazeotropic distillation of the F and AA recovery process (cf. Fig. 2; $p = 20$ kPa, the column feed is specified in Tab. 4). N is the total number of stages and \dot{Q}_R is the reboiler duty.

5 Results and Discussion

The stream table and heat duties for the design point of the F recovery process (Fig. 1) are presented in Tabs. 3 and 5, respec-

Table 3. Simulation results for the stream table of the F recovery process. The number of equilibrium stages of the distillation column is $N = 8$.

Stream	T [K]	\dot{m} [kg h ⁻¹]	W		X		AA		F	
			\dot{m}_i [kg h ⁻¹]	$x_i^{(m)}$ [g g ⁻¹]	\dot{m}_i [kg h ⁻¹]	$x_i^{(m)}$ [g g ⁻¹]	\dot{m}_i [kg h ⁻¹]	$x_i^{(m)}$ [g g ⁻¹]	\dot{m}_i [kg h ⁻¹]	$x_i^{(m)}$ [g g ⁻¹]
FEED	298.15	2000.000	1776.000	0.888	142.000	0.071	24.000	0.012	58.000	0.029
L	334.00	601.308	447.975	0.745	141.909	0.236	8.418	0.014	3.006	0.005
V	334.00	1398.692	1325.960	0.948	0.000	0.000	16.784	0.012	55.948	0.040
B	333.15	1350.320	1324.664	0.981	0.000	0.000	16.204	0.012	9.452	0.007
D	332.80	1398.758	1237.847	0.885	0.000	0.000	0.054	3.9×10^{-5}	160.857	0.115
R	298.15	1350.386	1235.550	0.915	0.000	0.000	0.053	3.9×10^{-5}	114.783	0.085
P	298.15	48.3720	2.515	0.052	0.000	0.000	0.001	3.1×10^{-5}	45.856	0.948

Table 4. Simulation results for the F and AA recovery process. $N = 28$; $N_S = 20$; $N_F = 20$; flow rate of the side draw, $\dot{m}_S = 1333.91$ kg h⁻¹; $\dot{Q}_R = 2330.78$ kW.

Stream	T [K]	\dot{m} [kg h ⁻¹]	W		X		AA		F	
			\dot{m}_i [kg h ⁻¹]	$x_i^{(m)}$ [g g ⁻¹]	\dot{m}_i [kg h ⁻¹]	$x_i^{(m)}$ [g g ⁻¹]	\dot{m}_i [kg h ⁻¹]	$x_i^{(m)}$ [g g ⁻¹]	\dot{m}_i [kg h ⁻¹]	$x_i^{(m)}$ [g g ⁻¹]
FEED	298.15	2000.000	1776.000	0.888	142.000	0.071	24.000	0.012	58.000	0.029
L	334.00	601.308	447.975	0.744	141.909	0.236	8.418	0.014	3.006	0.005
V	334.00	1398.692	1325.960	0.949	0.000	0.000	16.784	0.012	55.948	0.040
B	341.30	9.110	0.455	0.05	0.000	0.000	8.655	0.95	0.000	0.000
S	333.20	1334.023	1323.351	0.992	0.000	0.000	8.004	0.006	2.668	0.002
D	332.90	5006.93	4531.177	0.905	0.000	0.000	0.095	1.9×10^{-5}	475.658	0.095
R	298.15	4951.371	4530.411	0.915	0.000	0.000	0.094	1.9×10^{-5}	420.866	0.085
P	298.15	55.559	2.889	0.052	0.000	0.000	0.001	1.5×10^{-5}	52.669	0.948

Table 5. Heat duties [kW] for the F recovery process (column labeled 1) and for the F and AA recovery process (column labeled 2).

	1	2
Evaporator	957.46	957.46
Condenser	881.53	3212.35
Reboiler	–	2330.78

tively; the corresponding results for the F and AA recovery process (Fig. 2) are presented in Tabs. 4 and 5. Feed stream and specifications are in the range that is interesting for industrial applications.

The FEED of the process is an aqueous solution of X with a molarity of X of 80 g L^{-1} that also contains AA and F in low concentration (mass fractions: 0.029 g g^{-1} F and 0.012 g g^{-1} AA). The feed flow rate was chosen to be 2000 kg h^{-1} . The concentration step should yield a concentration of X of at least 300 g L^{-1} . In the present design, the evaporation rate is 70 % of the feed stream, leading to a concentration of X of 309 g L^{-1} in stream L. At the chosen pressure of 20.0 kPa, the temperature in the evaporator is 344 K, which is sufficiently low to prevent thermal degradation of X.

During partial evaporation, the mass fraction of F is reduced from 0.029 g g^{-1} in FEED to 0.005 g g^{-1} in stream L. FEED contains 58 kg h^{-1} F, of which 55.95 kg h^{-1} are evaporated, corresponding to 96.5 %. For AA, the results are less favorable: the mass fraction in FEED is 0.012 g g^{-1} , which increases slightly upon partial evaporation to 0.014 g g^{-1} . Nevertheless, from 24 kg h^{-1} AA in FEED, 16.78 kg h^{-1} are evaporated, corresponding to 69.9 %.

The concentrations of both AA and F in stream L are above the levels that are typically accepted for fermentation, such that additional detoxification steps are needed. These detoxification steps are, however, facilitated by the substantial removal of F and AA during evaporation. The evaporation unit is the same for both processes discussed herein.

In the F recovery process (Fig. 1 and Tabs. 3 and 5), F is recovered with a purity of almost 0.95 g g^{-1} (stream P). The remaining 0.05 g g^{-1} are basically W; only traces of AA are found. The losses of F in the distillation column are about 9 kg h^{-1} , due to the absence of a stripping section. Nevertheless, the overall F recovery rate of the process (including evaporation and distillation) is almost 80 %. The bottom stream of the distillation is W with a purity of 0.98 g g^{-1} ; the rest is F and AA. In the process, heat is only supplied to the evaporator. The heat duty for the single-effect system studied herein is about 960 kW. The distillation column required for the recovery of F is a small distillation column with just eight equilibrium stages and without a stripping section. The heat duty is zero; there is no additional operational expenditure. The low capital expenditure for the small column and the fact that F is a valuable chemical make the new F recovery process economically attractive.

In contrast, in the F and AA recovery process (Fig. 2, Tabs. 4 and 5), not only is a heat duty of 960 kW needed for evaporation, but also an additional 2330 kW for the reboiler. The

amount of AA recovered is only 9 kg h^{-1} , which corresponds to an overall recovery rate of AA of about 40 %. There are only minor changes regarding the recovery of F, relative to the simple process discussed above. This shows that AA recovery by distillation is feasible, but completely unattractive.

6 Conclusions

The integration of the concentration and detoxification of wood hydrolysates by evaporation, with the recovery of the valuable inhibitors F and AA by distillation, was studied. Computer simulations were performed for a quaternary system (W + X + AA + F) chosen to represent the hydrolysate. It was shown that it is possible to recover F by heteroazeotropic distillation without having to use additional energy, relative to a single evaporation step, because even without the recovery of F vapor from the evaporator would have to be condensed. Also, the recovery of AA by distillation is possible, but the process is economically not attractive.

Simulations reported herein were based on a thermodynamic model of the system (W + X + AA + F) that was thoroughly tested in a previous study [16]. However, the studied mixture is only a model system; real hydrolysates contain many additional components. Additional experimental studies with real hydrolysates should be performed to validate the process concept. Furthermore, there is some arbitrariness in the specifications of the feed and the product purity used for the present case study. Additional simulations were performed, which showed that the design was feasible and robust for a wide range of choices of these parameters. The energy demand of the process could be reduced by using multiple effects for evaporation. This has important consequences for the integration of the recovery of F because less steam is available. By using the model presented herein, these options can also be studied easily.

Acknowledgment

This research project has received funding from the European Union's (EU's) framework programme for research and innovation Horizon 2020 (2014–2020) under grant agreement no. 636077.

The authors have declared no conflict of interest.

Symbols used

a	[–]	NRTL binary interaction parameter
b	[K]	NRTL binary interaction parameter
K	[–]	thermodynamic equilibrium constant
\dot{m}	[kg h^{-1}]	flow rate
N	[–]	number of equilibrium stages
p	[kPa]	pressure
Q	[kW]	heat duty
T	[K]	temperature
x_i	[mol mol^{-1}]	mole fraction of component i
$x_i^{(m)}$	[g g^{-1}]	mass fraction of component i

y [mol mol⁻¹] vapor-phase mole fraction of acetic acid

Greek letters

α [-] NRTL nonrandomness parameter
 τ [-] NRTL binary interaction parameter

Sub- and superscripts

D dimerization reaction of acetic acid in the vapor phase
F feed
 i component i
 j component j
R reboiler
s vapor
S side draw

Abbreviations

AA acetic acid
B bottom stream
COL distillation column
D distillate stream
DEC decanter
EVAP evaporator
F furfural
L liquid stream exiting the evaporator
LLE liquid-liquid equilibrium
NRTL nonrandom two-liquid activity coefficient model
P product stream
R reflux stream
S side draw
V vapor stream exiting the evaporator
VLE vapor-liquid equilibrium
VLLE vapor-liquid-liquid equilibrium
W water
X xylose

References

- [1] F. Cherubini, *Energy Convers. Manage.* **2010**, *51* (7), 1412–1421. DOI: <https://doi.org/10.1016/j.enconman.2010.01.015>
- [2] G. W. Huber, A. Corma, *Angew. Chem., Int. Ed.* **2007**, *46* (38), 7184–7201. DOI: <https://doi.org/10.1002/anie.200604504>
- [3] J. Burger, E. Ströfer, H. Hasse, *Chem. Eng. Technol.* **2016**, *39* (2), 219–224. DOI: <https://doi.org/10.1002/ceat.201500196>
- [4] F. H. Isikgor, C. R. Becer, *Polym. Chem.* **2015**, *6* (25), 4497–4559. DOI: <https://doi.org/10.1039/c5py00263j>
- [5] M. Valdivia, J. L. Galan, J. Laffarga, J.-L. Ramos, *Microb. Biotechnol.* **2016**, *9* (5), 585–594. DOI: <https://doi.org/10.1111/1751-7915.12387>
- [6] A. Limayem, S. C. Ricke, *Prog. Energy Combust. Sci.* **2012**, *38* (4), 449–467. DOI: <https://doi.org/10.1016/j.pecs.2012.03.002>
- [7] L. Olsson, B. Hahn-Hägerdal, *Enzyme Microb. Technol.* **1996**, *18* (5), 312–331. DOI: [https://doi.org/10.1016/0141-0229\(95\)00157-3](https://doi.org/10.1016/0141-0229(95)00157-3)
- [8] J.-P. Lange, E. van der Heide, J. van Buijtenen, R. Price, *ChemSusChem* **2012**, *5* (1), 150–166. DOI: <https://doi.org/10.1002/cssc.201100648>
- [9] L. J. Jönsson, B. Alriksson, N.-O. Nilvebrant, *Biotechnol. Biofuels* **2013**, *6* (16), 1–10. DOI: <https://doi.org/10.1186/1754-6834-6-16>
- [10] E. Palmqvist, B. Hahn-Hägerdal, *Bioresour. Technol.* **2000**, *74* (1), 17–24. DOI: [https://doi.org/10.1016/S0960-8524\(99\)00160-1](https://doi.org/10.1016/S0960-8524(99)00160-1)
- [11] S. Larsson, A. Reimann, N.-O. Nilvebrant, L. J. Jönsson, *Appl. Biochem. Biotechnol.* **1999**, *77* (1), 91–103. DOI: <https://doi.org/10.1385/ABAB:77:1-3:91>
- [12] C. Vila, V. Santos, J. C. Parajó, *Bioresour. Technol.* **2003**, *90* (3), 339–344. DOI: [https://doi.org/10.1016/S0960-8524\(03\)00030-0](https://doi.org/10.1016/S0960-8524(03)00030-0)
- [13] A. K. Chandel, S. S. da Silva, O. V. Singh, in *Biofuel Production – Recent Developments and Prospects*, InTech, Rijeka **2011**, Ch. 10, 225–246. DOI: <https://doi.org/10.5772/16454>
- [14] L. Fele, V. Grilc, *J. Chem. Eng. Data* **2003**, *48* (3), 564–570. DOI: <https://doi.org/10.1021/je020117y>
- [15] S. Yi, X. Qingruo, W. Tengyou, T. Zhangfa, *CIESC J.* **2011**, *62* (7), 1800–1807. DOI: <https://doi.org/10.3969/j.issn.0438-1157.2011.07.003>
- [16] N. Galeotti, *Ph.D. Thesis*, in preparation, Technical University of Kaiserslautern **2019**.
- [17] H. Renon, J. M. Prausnitz, *AIChE J.* **1968**, *14* (1), 135–144. DOI: <https://doi.org/10.1002/aic.690140124>
- [18] *Aspen Plus V8.6, aspenONE*, Aspen Technology, Inc., Bedford, MA **2014**.
- [19] S. Zeck, *Chem. Ing. Tech.* **1990**, *62* (9), 707–717. DOI: <https://doi.org/10.1002/cite.330620904>